OPEN

^{18}F-Fluorodeoxyglucose Positron Emission Tomography/Magnetic Resonance in Lymphoma

Comparison With ^{18}F-Fluorodeoxyglucose Positron Emission Tomography/Computed Tomography and With the Addition of Magnetic Resonance Diffusion-Weighted Imaging

Chiara Giraudo, MD,* Markus Raderer, MD,† Georgios Karanikas, MD,* Michael Weber, PhD,*
Barbara Kiesewetter, MD,† Werner Dolak, MD,‡
Ingrid Simonitsch-Klupp, MD,§ and Marius E. Mayerhoefer, MD, PhD*

Objectives: The aim of this study was to compare ^{18}F-fluorodeoxyglucose (FDG) positron emission tomography (PET)/magnetic resonance (MR) (with and without diffusion-weighted imaging [DWI]) to ^{18}F-FDG PET/computed tomography (CT), with regard to the assessment of nodal and extranodal involvement, in patients with Hodgkin lymphoma and non-Hodgkin lymphoma, without restriction to FDG-avid subtypes.

Materials and Methods: Patients with histologically proven lymphoma were enrolled in this prospective, institutional review board–approved study. After a single ^{18}F-FDG injection, patients consecutively underwent ^{18}F-FDG PET/CT and ^{18}F-FDG PET/MR on the same day for staging or restaging. Three sets of images were analyzed separately: ^{18}F-FDG PET/CT, ^{18}F-FDG PET/MR without DWI, and ^{18}F-FDG PET/MR with DWI. Region-based agreement and examination-based sensitivity and specificity were calculated for ^{18}F-FDG PET/CT, ^{18}F-FDG PET/MR without DWI, and ^{18}F-FDG PET/MR DWI. Maximum and mean standardized uptake values (SUV$_{max}$, SUV$_{mean}$) on ^{18}F-FDG PET/CT and ^{18}F-FDG PET/MR were compared and correlated with minimum and mean apparent diffusion coefficients (ADC$_{min}$, ADC$_{mean}$).

Results: Thirty-four patients with a total of 40 examinations were included. Examination-based sensitivities for ^{18}F-FDG PET/CT, ^{18}F-FDG PET/MR, and ^{18}F-FDG PET/MR DWI were 82.1%, 85.7%, and 100%, respectively; specificities were 100% for all 3 techniques; and accuracies were 87.5%, 90%, and 100%, respectively. ^{18}F-FDG PET/CT was false negative in 5 of 40 examinations (all with mucosa-associated lymphoid tissue lymphoma), and ^{18}F-FDG PET/MR (without DWI) was false negative in 4 of 40 examinations. Region-based percentages of agreement were 99% (κ, 0.95) between ^{18}F-FDG PET/MR DWI and ^{18}F-FDG PET/CT, 99.2% (κ, 0.96) between ^{18}F-FDG PET/MR and ^{18}F-FDG PET/CT, and 99.4% (κ, 0.97) between ^{18}F-FDG PET/MR DWI and ^{18}F-FDG PET/MR. There was a strong correlation between ^{18}F-FDG PET/CT and ^{18}F-FDG PET/MR for SUV$_{max}$ ($r = 0.83$) and SUV$_{mean}$ ($r = 0.81$) but no significant correlation between ADC$_{min}$ and SUV$_{max}$ (^{18}F-FDG PET/CT: $r = 0.46$, $P = 0.65$; ^{18}F-FDG PET/MR: $r = 0.64$, $P = 0.53$) or between ADC$_{mean}$ and SUV$_{mean}$ (respectively, $r = -0.14$, $P = 0.17$ for the correlation with PET/CT and $r = -0.14$, $P = 0.14$ for the correlation with PET/MR).

Conclusions: ^{18}F-FDG PET/MR and ^{18}F-FDG PET/CT show a similar diagnostic performance in lymphoma patients. However, if DWI is included in the ^{18}F-FDG PET/MR protocol, results surpass those of ^{18}F-FDG PET/CT because of the higher sensitivity of DWI for mucosa-associated lymphoid tissue lymphomas.

Key Words: ^{18}F-FDG PET/MR, DWI, lymphoma

(*Invest Radiol* 2016;51: 163–169)

Imaging plays a critical role in both the initial staging and restaging of lymphomas. While ^{18}F-fluorodeoxyglucose (FDG) positron emission tomography (PET)/computed tomography (CT) is well established as the imaging technique of choice for the assessment of patients with Hodgkin lymphoma (HL) and the majority of non-Hodgkin lymphomas (NHLs),[1–6] whole-body magnetic resonance imaging (MRI) has been proposed as an alternative to ^{18}F-FDG PET/CT, in particular if MR diffusion-weighted imaging (DWI) is part of the protocol.[7–13] At present, PET/CT is generally regarded as moderately superior to MRI with DWI, especially for nodal staging (partly due to motion artifacts that may occur in the head and neck region as well as the mediastinum), whereas DWI is considered superior to some indolent NHL subtypes, such as extranodal marginal zone B-cell lymphoma of the mucosa-associated lymphoid tissue (MALT), which are frequently not FDG avid.[12,13]

Whole-body ^{18}F-FDG PET/MR has only recently been introduced into routine clinical imaging,[14–16] and thus, its role in diagnosing lymphoma is still largely unknown. ^{18}F-FDG PET/MR offers not only a combination of metabolic information (provided by ^{18}F-FDG PET) with high soft tissue contrast anatomic resolution (provided by morphological MRI), but also enables, through the use of DWI, an indirect assessment of cell density.

Only 3 studies have been published with regard to the value of ^{18}F-FDG PET/MR for assessing HL and NHL; as yet, one of them included only nodal lymphoma manifestations and did not include DWI at all[17]; another study focused exclusively on therapy response and only applied DWI in 2 patients.[18] The most recent study included DWI, but only as a stand-alone technique, rather than as part of the ^{18}F-FDG PET/MR protocol.[19] Furthermore, none of these studies included a relevant number of lymphomas with variable FDG avidity, such as MALT lymphoma, even though, for instance, the latter is the third most common NHL subtype.

Thus, it was the aim of our study to directly and prospectively compare ^{18}F-FDG PET/MR, including DWI, to ^{18}F-FDG PET/CT, with regard to the assessment of nodal and extranodal involvement, in lymphoma patients, without restriction to FDG-avid subtypes.

MATERIALS AND METHODS

Patients and Study Design

Between January 2014 and April 2015, patients with histologically proven lymphoma (as verified by a reference pathologist who

analyzed tissue samples obtained by biopsy or surgery, according to the current World Health Organization classification of hematological and lymphoid malignancies), who were referred to the local tertiary care center for pretherapeutic staging or follow-up, were invited to participate in this single-tracer injection, dual-modality study. The study was approved by the local institutional review board. Patients who gave written informed consent underwent ^{18}F-FDG PET/CT and, directly after it, ^{18}F-FDG PET/MR (see protocols below). Pregnancy, general contraindications to MRI (eg, claustrophobia, metal implants), elevated glucose levels (>150 mg/dL), and known adverse reactions to ionized contrast media were used as exclusion criteria.

Imaging Protocols

^{18}F-FDG PET/CT and ^{18}F-FDG PET/MR were performed consecutively on the same day, using only a single injection of ^{18}F-FDG for both examinations.

^{18}F-FDG PET/CT was generally performed first, covering the anatomy from the vertex to the upper thigh, using a 64-row multidetector hybrid PET/CT device (Biograph TruePoint 64; Siemens, Erlangen, Germany). For PET, this scanner offers an axial field of view (FOV) of 216 mm, a sensitivity of 7.6 cps/kBq, and a transaxial resolution of 4 to 5 mm. After patients had fasted for 5 hours, PET was performed 45 to 60 minutes after an intravenous administration of 300 MBq of ^{18}F-FDG, with 3 minutes/bed position, 4 iterations, 21 subsets, a 5-mm slice thickness, and a 168×168 matrix, using the point-spread function–based reconstruction algorithm TrueX. Venous-phase contrast-enhanced (CE) CT was used for attenuation correction and was obtained after the intravenous injection of 100 mL of a tri-iodated, nonionic contrast medium at a rate of 2 mL/s; a tube voltage of 120 mA; a tube current of 230 kV; a collimation of 64×0.6 mm; a 3-mm slice thickness with a 2-mm increment; and a 512×512 matrix. Contrast-enhanced CT was used instead of unenhanced CT because, as well demonstrated in the literature, the administration of contrast medium improves the evaluation of extranodal disease and better delineates lymph node stations.[20]

^{18}F-FDG PET/MR, covering the same anatomy as the PET/CT, was performed directly after PET/CT, using an integrated, simultaneous, hybrid PET/MR device (Biograph mMR; Siemens, Erlangen, Germany) operating at 3 T, with high-performance gradient systems (45 mT/m) and a slew rate of 200 T/m/s, and equipped with a phased-array body coil. For PET, the system offers an axial FOV of 256 mm, a sensitivity of 13.2 cps/kBq, and a transaxial resolution of 4.4 mm. Positron emission tomography was performed 100 to 150 minutes after the original tracer administration, with 5 minutes/bed position, 3 iterations, 21 subsets, a 4.2-mm slice thickness, and a 172×172 matrix, using the point-spread function–based reconstruction algorithm High Definition-PET. An axial, 2-point Dixon, 3-dimensional, volume-interpolated, T1-weighted breath-hold MR sequence (VIBE) was acquired for attenuation correction and for anatomic correlation, using the following parameters: repetition time (TR)/echo times (TE), 4.02/1.23, 2.46 milliseconds; 1 average, 2 echoes; a 10-degree flip angle; a 320×175 matrix with a 430×309 mm FOV; and a 3-mm slice thickness with 0.6-mm gap. A coronal T2-weighted half-fourier acquisition single-shot turbo spin-echo (HASTE) was performed applying the following parameters: TR/TE, 1400/121 milliseconds; a 108-degree flip angle; a 256×256 matrix with a 380×380 mm FOV; and a 6-mm slice thickness with a 1.2-mm gap. A single-shot, echo planar imaging–based, spectral adiabatic inversion recovery DWI sequence was obtained with the following parameters: b-values, 50 and 800; TR/TE, 6800/63 milliseconds; 6 averages and 1 echo; a 180-degree flip angle; a 168×104 matrix with a 440×340 mm FOV; and a 6-mm slice thickness with a 1.2-mm gap. The total scanning time for entire PET/MR examination was ~120 minutes, including ~15 to 20 minutes for the DWI sequence.

Image Analysis

The 14 nodal regions defined at the Rye symposium[21] and the following 12 extranodal regions were evaluated: Waldeyer ring, lungs,

liver, spleen, stomach, small intestine, large intestine, right kidney, left kidney, bones, soft tissues (skin/fat/muscle), and other organs/tissues (eg, salivary glands). A patient was rated positive if at least 1 region was positive. Staging, according to the modified Ann Arbor system (stage I to IV),[3,22] was performed for all pretherapeutic staging examinations. In addition, stage 0 was reported for cases rated as negative (ie, negative at imaging and/or at the reference standard). A board-certified radiologist and a board-certified nuclear medicine physician, who were blinded to the clinical and histological information, performed all analyses in consensus.

^{18}F-FDG PET/CT

Positron emission tomography/CT was rated as positive if at least one of the nodal or extranodal regions demonstrated 1 or more focally increased tracer accumulations relative to the surrounding tissues or mediastinal blood pool activity (for staging) or to the liver (for restaging).[2] Contrast-enhanced CT was used for anatomical correlation and (in case of lymph nodes) morphological verification. In accordance with the Lugano classification,[2] the spleen and liver were also rated as positive if there was a diffusely increased FDG uptake.

In the absence of abnormal ^{18}F-FDG PET findings, lymph nodes were also rated as positive, using CE-CT, if they met the size criteria defined by the International Working Group[20]: a long-axis diameter of more than 1.5 cm or a long-axis and short-axis diameter of more than 1 cm each.[20] The spleen was rated as positive if its vertical diameter was greater than 13 cm.[2] No other size criteria were applied for extranodal regions, and all noncystic, nonfatty lesions (ie, Hounsfield units greater than 20) on CE-CT were rated as positive for lymphoma, unless they showed well-established benign features (eg, nodular peripheral enhancement in hemangiomas of the liver).

^{18}F-FDG PET/MR Without DWI

For ^{18}F-FDG PET/MR without DWI, PET criteria were identical to those applied for PET/CT (see above). T1-weighted and T2-weighted MRI were used for morphological correlation of abnormal tracer accumulations on ^{18}F-FDG PET. The vertical diameter of the spleen—considered abnormal if greater than 13 cm—was assessed on coronal T2 HASTE MRI.

^{18}F-FDG PET/MR With DWI

For ^{18}F-FDG PET/MR DWI (ie, PET/MR with DWI), PET criteria for lymphoma involvement were identical to those used for ^{18}F-FDG PET/MR without DWI (see above). In the absence of pathological PET findings, however, nodal and extranodal regions were also rated as positive if there was a lesion with restricted diffusion, that is, with a high signal on b800 DWI and a low signal on the corresponding apparent diffusion coefficient (ADC) map.[23] Because false-positive findings in lymph nodes have been previously reported with DWI,[24] only lymph nodes with restricted diffusion that had a long axis diameter of more than 1 cm were rated as positive. The spleen was rated as positive if the vertical diameter was greater than 13 cm,[2] as assessed on coronal T2 HASTE MRI, or if DWI showed evident signal inhomogeneity or well-circumscribed lesions with restricted diffusion.[25,26] Bone and bone marrow were rated as positive if, in addition to a focal or diffuse diffusion restriction, there was also a low signal on T1-weighted MRI.[12]

Quantitative Analysis

For each nodal and extranodal region rated as positive, the lesion demonstrating the largest diameter was selected, and the maximum and mean standardized uptake value (SUV_{max} and SUV_{mean}), assessed independently on ^{18}F-FDG PET/CT and ^{18}F-FDG PET/MR, as well as the minimum and the mean ADC ($\times 10^{-6}$ mm^2/s), were measured. For the SUV measurements, isocontour volumes of interest that included

TABLE 1. Demographic Data for the 34 Lymphoma Patients

Sex, male/female	19/15
Age, mean (SD), y	56 (19.23)
Histology	
MALT	15
MCL	5
Hodgkin	4
MZL	3
Burkitt	2
Follicular lymphoma	2
Diffuse large B-cell lymphoma	2
T-cell lymphoma	1
Staging/restaging	16/18*

*Thirty-four patients with 40 examinations (6 patients scanned twice: 3 for staging and restaging and 3 twice for restaging).

MALT indicates mucosa-associated lymphoid tissue; MCL, mantle cell lymphoma; MZL, marginal zone lymphoma.

all voxels more than 50% of the SUV_{max} of each lesion, were used. However, ADC measurements were based on regions of interest that were manually defined[27] on the ADC map section that showed the maximum transverse diameter of a lesion. All quantitative measurements were performed by the same rater.

Reference Standard and Statistical Analysis

For staging, histology was used as the main reference standard and was required for all extranodal lymphoma manifestations. For suspected lymph node involvement, histological verification in at least a single nodal region was required. In case of involvement of multiple nodal regions, positive findings on both ^{18}F-FDG PET and DWI were required to verify each non–histologically proven region (combined reference standard). The combined reference standard was also used for posttreatment restaging, unless rebiopsy was performed—in the latter case, the main reference standard was used on a per-region basis.

To determine the diagnostic values of ^{18}F-FDG PET/MR, ^{18}F-FDG PET/MR DWI, and ^{18}F-FDG PET/CT, examination-based sensitivity, specificity, and accuracy, as well as their 95% confidence intervals (CIs), were calculated. κ Coefficients were used to assess the region-based agreement and the agreement for the modified Ann Arbor Staging system. Spearman correlation coefficients (r) were used to

assess the relationship between SUVs and ADCs. The specified level of significance was $P \leq 0.05$ for all tests. All statistical tests were performed using IBM SPSS Statistics 21.0 (IBM Corp, Armonk, NY).

RESULTS

Thirty-four patients (19 males and 15 females; mean [SD] age, 56 [19.23] years) met our criteria for participation in the study. Histology revealed HL in 4 patients, aggressive NHL in 10 patients, and indolent NHL in 20 patients (Table 1). Six patients were scanned twice: 3 underwent both staging and restaging, and 3 were scanned twice for restaging. Thus, 40 examinations were available for analysis.

All ^{18}F-FDG PET/CT and ^{18}F-FDG PET/MR (−DWI) examinations were successfully performed, without any interruptions. All sets of images generally had a high quality, allowing accurate qualitative and quantitative analysis; nevertheless, 4 regions had to be excluded from the quantitative measurements due to artifacts on ^{18}F-FDG PET/MR (ie, both T1 and DWI images were corrupted).

Examination-Based Assessment

Examination-based sensitivities for ^{18}F-FDG PET/CT, ^{18}F-FDG PET/MR, and ^{18}F-FDG PET/MR DWI were 82.1%, 85.7%, and 100%, respectively, whereas specificities were 100% for all 3 techniques, and accuracies were 87.5%, 90%, and 100%, respectively (Table 2). ^{18}F-FDG PET/CT was false negative in 5 of 40 examinations (ie, 4 MALT lymphoma patients, one of them scanned for staging and restaging) (Fig. 1). ^{18}F-FDG PET/MR (without DWI) was false negative in 4 of 40 examinations (ie, these 4 lesions were biopsy proven); notably, 1 gastric MALT lymphoma showed no pathologic FDG uptake at ^{18}F-FDG PET/CT but did show pathologic FDG uptake on ^{18}F-FDG PET/MR. There were no false-positive or false-negative findings on ^{18}F-FDG PET/MR DWI—indeed, all 28 examinations that were positive according to the reference standard demonstrated at least 1 lesion with pathologic FDG uptake or restricted diffusion.

Ann Arbor Staging

On ^{18}F-FDG PET/MR DWI, 3 of 16 patients available for staging were negative (stage 0), 4 of 16 were rated as stage I, 3 of 16 as stage II, 1 of 16 as stage III, and 5 of 16 as stage IV. Two of 3 patients that showed stage I disease on ^{18}F-FDG PET/MR DWI (histologically proven MALT lymphomas of the bladder, stomach, and duodenum) were false negative (stage 0) on both ^{18}F-FDG PET/MR and ^{18}F-FDG PET/CT, whereas the remaining patient was rated negative only on the latter. Thus, agreements between ^{18}F-FDG PET/MR DWI and ^{18}F-FDG PET/MR and ^{18}F-FDG PET/CT, in terms of staging, were high,

TABLE 2. Examination-Based Performances of ^{18}F-FDG PET/CT, ^{18}F-FDG PET/MR, and ^{18}F-FDG PET/MR DWI

Reference Standard

		Pos	Neg	Total	Se (95% CI), %	Sp (95% CI), %	Ac (95% CI), %
PET/CT	Pos	23	0	23	82.1 (64.4–92.1)	100 (75.7–100)	85.7 (73.9–94.5)
	Neg	5	12	17			
	Total	28	12	40			
PET/MR	Pos	24	0	24	85.7 (68.5–94.3)	100 (75.7–100)	90 (76.9–96)
	Neg	4	12	16			
	Total	28	12	40			
PET/MR DWI	Pos	28	0	28	100 (87.9–100)	100 (75.7–100)	100 (91.2–100)
	Neg	0	12	12			
	Total	28	12	40			

FDG indicates fluorodeoxyglucose; PET, positron emission tomography; CT, computed tomography; MR, magnetic resonance; DWI, diffusion-weighted imaging; Pos, number of positive examinations; Neg, number of negative examinations; Se, sensitivity; CI, confidence interval; Sp, Specificity; Ac, accuracy.
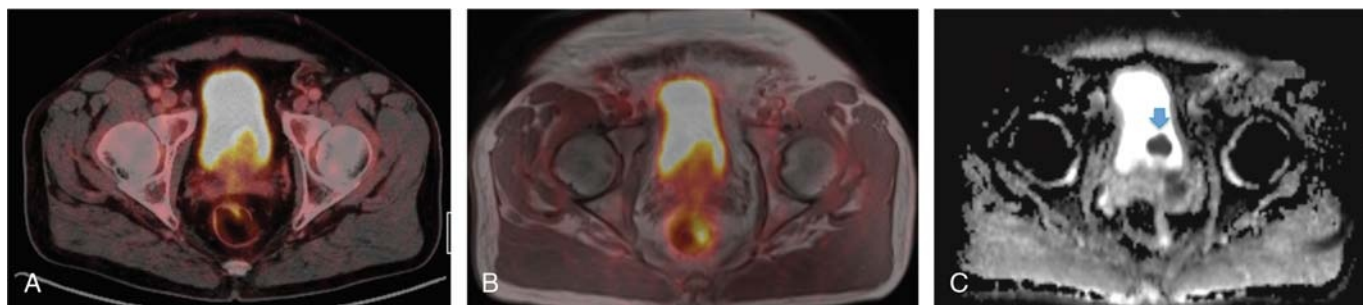
FIGURE 1. A 69-year-old male patient with a histologically verified MALT lymphoma of the bladder. On the color-coded, fused ^{18}F-FDG PET/CT (A) and ^{18}F-FDG PET/MR (B) images, no increased tracer uptake is visible. However, the ADC map (C) clearly shows the extranodal lymphoma involvement (light blue arrow).

with κ values of 0.84 and 0.76, respectively; the agreement between ^{18}F-FDG PET/MR and ^{18}F-FDG PET/CT was even higher (κ, 0.92).

Region-Based Agreement

Overall, 1036 of 1040 regions were available for comparative analysis; the remaining 4, as aforementioned, were excluded due to artifacts on ^{18}F-FDG PET/MR. A total of 113, 107, and 105 regions were positive on ^{18}F-FDG PET/MR DWI, ^{18}F-FDG PET/MR, and ^{18}F-FDG PET/CT, respectively (Table 3; Figs. 2, 3).

Of the 9 extranodal lesions (ie, 8 MALT lymphoma manifestations of the liver, stomach, duodenum, and bladder, and 1 bone marrow manifestation in a marginal zone lymphoma [MZL] patient) that were positive on ^{18}F-FDG PET/MR DWI, but negative on ^{18}F-FDG PET/CT, 6 were also negative on ^{18}F-FDG PET/MR. The remaining 3 lesions (1 gastric and 1 hepatic lesion; the latter scanned at both staging and restaging) were found in MALT lymphoma patients and demonstrated a pathologic FDG uptake on ^{18}F-FDG PET/MR but not on ^{18}F-FDG PET/CT. Three nodal regions in a patient affected by mantle cell lymphoma (MCL) did not show any pathologic FDG uptake at ^{18}F-FDG PET/MR, and one (a mediastinal lymph node) was also negative on ^{18}F-FDG PET/MR DWI. Accordingly, percentages of agreement were 99% (95% CI, 98.5%–99.6%; κ, 0.95) between ^{18}F-FDG PET/MR DWI and ^{18}F-FDG PET/CT, 99.2% (95% CI, 98.6%–99.7%; κ, 0.96) between ^{18}F-FDG PET/MR and ^{18}F-FDG PET/CT, and 99.4%

TABLE 3. Region-Based Lymphoma Assessment on ^{18}F-FDG PET/CT, ^{18}F-FDG PET/MR, and ^{18}F-FDG PET/MR DWI

Positive Regions*	Nodal	Extranodal	Total
PET/CT	77	28	105
PET/MR	74	33	107
PET/MR DWI	76	37	113

Region-Based Agreement*	κ Values
PET/CT vs PET/MR	0.96
PET/CT vs PET/MR DWI	0.95
PET/MR vs PET/MR DWI	0.97

*Total number of regions for comparative analysis, n = 1036/1040 (4 excluded due to artifacts on both T1 and DWI images).

FDG indicates fluorodeoxyglucose; PET, positron emission tomography; CT, computed tomography; MR, magnetic resonance; DWI, diffusion-weighted imaging.

(95% CI, 98.9%–99.8%; κ, 0.97) between ^{18}F-FDG PET/MR and ^{18}F-FDG PET/MR DWI (Table 3).

Quantitative Analysis

One hundred five lesions were included in the quantitative analysis. Mean ± SD SUV_{max} and SUV_{mean} values were 9.07 ± 5.87 and 5.48 ± 3.49 on ^{18}F-FDG PET/CT as well as 7.08 ± 5.33 and 4.62 ± 3.49 on ^{18}F-FDG PET/MR, respectively. Although SUV_{max} and SUV_{mean} differed significantly between ^{18}F-FDG PET/CT and ^{18}F-FDG PET/MR ($P < 0.001$, respectively), they showed a strong correlation ($r = 0.83$ and $r = 0.81$) that was statistically significant ($P < 0.001$).

Mean ± SD ADC_{min} and ADC_{mean} values were 598.28 ± 221.89 and 774.44 ± 221.89 $\times 10^{-6}$ mm^2/s. No statistically significant correlation emerged between ADC_{min} and SUV_{max} (^{18}F-FDG PET/CT: $r = 0.46$, $P = 0.65$; ^{18}F-FDG PET/MR: $r = 0.64$, $P = 0.53$) or between ADC_{mean} and SUV_{mean} (^{18}F-FDG PET/CT: $r = -0.14$, $P = 0.17$; ^{18}F-FDG PET/MR: $r = -0.15$, $P = 0.14$).

DISCUSSION

The results of our study—which is, to date, the largest of its kind, the first that also included a relevant number of lymphomas with variable FDG avidity, and also the first that specifically evaluated the effect of including DWI in the PET/MR protocol—clearly suggest that ^{18}F-FDG PET/CT and ^{18}F-FDG PET/MR generally show a comparable performance in patients with lymphoma. Thus, our results are in good accordance with the few previous studies that reported a similar diagnostic performance of the 2 techniques[17–19] in lymphoma patients, and also in general accordance with the results of previous comparative studies in other types of cancer.[15,28–30]

As mentioned previously, the present study did not, a priori, exclude certain lymphoma subtypes, such as MALT lymphomas, which frequently show low, or no, FDG uptake. This strategy for inclusion/exclusion of patients was chosen because, in clinical practice, staging by means of imaging tests is sometimes performed before surgery/biopsy or before histologic workup of the tissue blocks, and thus, patients with lymphomas with variable FDG avidity (eg, MALT lymphoma, splenic MZL, small lymphocytic lymphoma/chronic lymphocytic leukemia, enteropathy-associated T-cell lymphoma, and primary cutaneous anaplastic large T-cell lymphoma) may still routinely undergo ^{18}F-FDG PET/CT or ^{18}F-FDG PET/MR.

Our study results indicate that, under such clinical conditions, the addition of DWI to the ^{18}F-FDG PET/MR protocol may improve the examination-based sensitivity and accuracy of this hybrid imaging technique. Accordingly, ^{18}F-FDG PET/MR DWI was also superior to ^{18}F-FDG PET/CT in our study. Notably, with regard to Ann Arbor staging, ^{18}F-FDG PET/MR DWI correctly upstaged 3 patients with histologically verified lymphoma manifestations that were missed by ^{18}F-FDG PET/CT. The latter results seem plausible because a previous
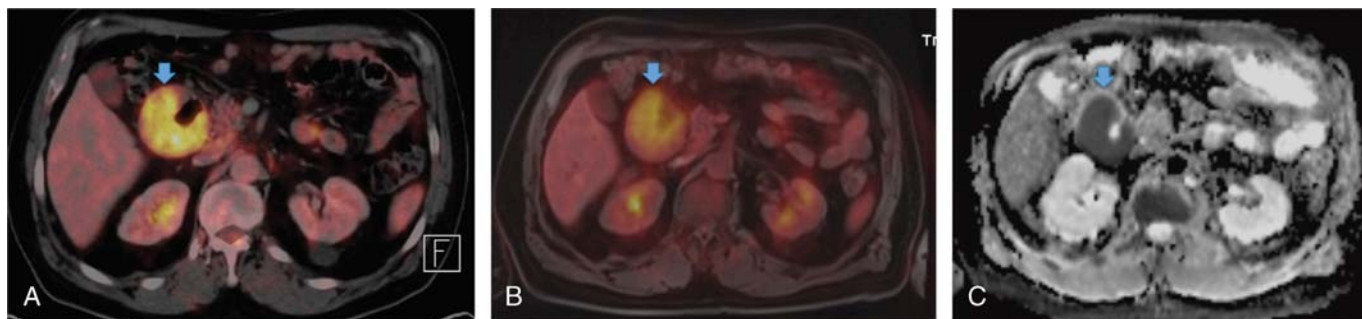
FIGURE 2. A 59-year-old male patient with a histologically verified MCL with nodal and extranodal manifestations. The color-coded, fused ^{18}F-FDG PET/CT (A) and ^{18}F-FDG PET/MR (B) images, as well as the ADC maps (C), clearly demonstrate the duodenal lymphoma involvement (light blue arrows).

study that compared (stand-alone) DWI-MRI to ^{18}F-FDG PET/CT, as well as CE-CT, reported a superiority of DWI-MRI in indolent NHLs with variable FDG avidity.[12]

However, the effect of including DWI in the ^{18}F-FDG PET/MR protocol would almost certainly not be as pronounced in a typical lymphoma population as it was in our study: 15 of 34 of our patients were diagnosed with MALT lymphoma, although this lymphoma subtype, while the third most common NHL, is normally responsible for just 7% to 8% of all NHLs.[31] By contrast, only 4 of 34 patients were diagnosed with the 2 most common types of NHL: diffuse large B-cell lymphoma (DLBCL) and follicular lymphoma. This highly atypical distribution of lymphoma subtypes within our sample is clearly due to the fact that one of the referring oncologists is an internationally recognized specialist for extranodal lymphomas, with a special focus on the MALT subtype.

With regard to region-based agreement, we noticed some discrepancies between the ^{18}F-FDG PET components of ^{18}F-FDG PET/CT and ^{18}F-FDG PET/MR. Two lesions in the liver (ie, 1 patient scanned twice and another patient scanned only once) and 1 gastric lesion in 2 patients with MALT lymphomas showed a pathological FDG uptake only on ^{18}F-FDG PET/MR, but not on ^{18}F-FDG PET/CT; whereas 3 lymph nodes in a patient with MCL showed a pathological FDG uptake only on ^{18}F-FDG PET/CT, but not on ^{18}F-FDG PET/MR. In the latter case, the ^{18}F-FDG PET/MR had—due to work flow reasons and contrary to the standard procedure—been performed before ^{18}F-FDG PET/CT. Heacock et al[19] reported a similar discrepancy

(ie, 1 hilar lymph node demonstrated a pathological FDG uptake on ^{18}F-FDG PET/MR but not on ^{18}F-FDG PET/CT). Because the authors also performed ^{18}F-FDG PET/MR after ^{18}F-FDG PET/CT, we hypothesize that the later time point used for the PET acquisition may be responsible for these findings. Indeed, delayed time point ^{18}F-FDG PET has already been demonstrated to improve the detection of colorectal and breast cancers,[32,33] as well as metastatic lymph nodes from lung and esophageal cancer.[34,35] A single study by Shinya et al[35] demonstrated that dual time point ^{18}F-FDG PET has the potential to provide a higher accuracy for the detection of aggressive lymphomas. Together with the aforementioned observation by Heacock et al, our findings suggest that the latter may also be true for indolent lymphomas. However, this topic was not within the scope of the present study, and thus, further studies are required to investigate this topic in detail.

With regard to quantitative measurements, several studies have already suggested an inverse correlation between SUV and ADC values.[36–38] SUV and ADC values are tumor biomarkers reflecting, respectively, tumor glucose metabolism (correlating with tumor grade) and tissue cellularity[39–41] (clinically applied to differentiate benign from malignant tumors and to assess tumor grade, delineate tumor extent, and predict survival). In our population, we observed substantial correlations of SUV_{max} and SUV_{mean} values between ^{18}F-FDG PET/MR and ^{18}F-FDG PET/CT, as also reported also by Heacock et al.[19] Recently, Punwani et al[42] demonstrated a significant negative correlation between ADC and SUV values, whereas in our study, the only
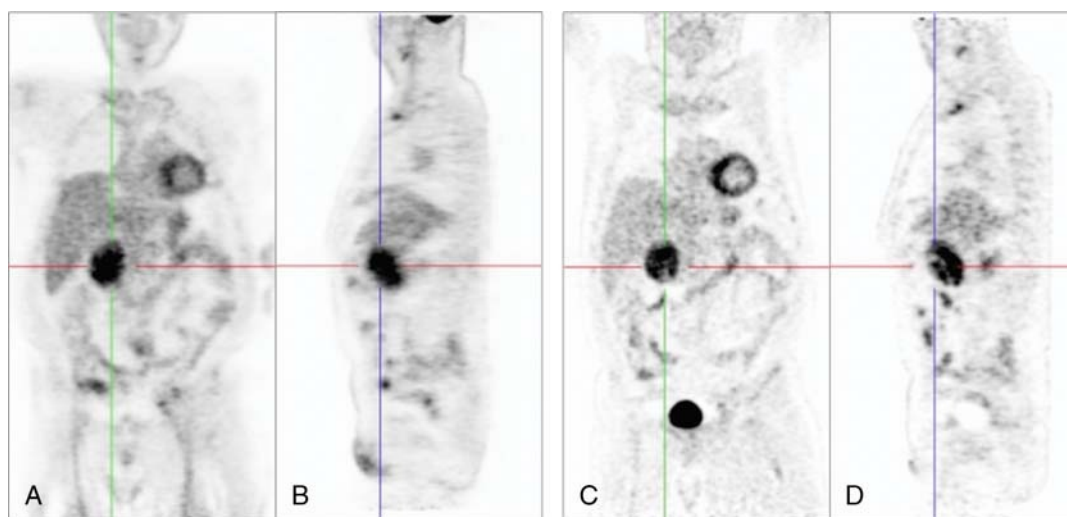

FIGURE 3. Coronal and sagittal maximum intensity projections of the same patient shown in Figure 2, based on the PET data obtained from ^{18}F-FDG PET/MR (A and B) and ^{18}F-FDG PET/CT (C and D). The duodenal lymphoma manifestations in the centers of the crosshairs show high ^{18}F-FDG uptake on all images.

significant correlation between these quantitative parameters was a weak negative correlation between SUV_{mean} and ADC_{mean}. This discrepancy may be due the fact that Punwani et al analyzed only a single lymphoma subtype (ie, Hodgkin). Notably, Heacock et al[19] and de Jong et al,[43] in their mixed lymphoma populations, also did not observe significant correlations between SUV and ADC values, and neither did Wu et al,[37] in patients with DLBCL. Thus, there seems to be no general relationship between glucose metabolism, as assessed by ^{18}F-FDG PET, and cell density, as assessed by DWI, across the entire spectrum of histological lymphoma subtypes.

The aforementioned, atypical distribution of lymphoma subtypes represents the main limitation of our study. However, combined with the results of previous, as well as future studies in patient populations with more typical lymphoma subtype distributions (ie, higher percentages of patients with HL, DLBCL, and follicular lymphoma), it may provide a well-rounded overview of the performance of ^{18}F-FDG PET/MR, compared with that of ^{18}F-FDG PET/CT, in this group of cancers. The fact that, on ^{18}F-FDG PET/MR DWI, we rated lesions as pathologic if they were positive on PET or DWI (ie, no agreement between the 2 was considered necessary) may be regarded as prone to overestimating the diagnostic performance of ^{18}F-FDG PET/MR DWI. However, we believe that, in general, the main strength of PET/MR lies in its multiparametric capabilities, and because the underlying information derived from ^{18}F-FDG PET (direct visualization of glucose metabolism at the cellular level) is quite different from that of DWI (indirect assessment of cell density), we believe that our evaluation strategy is justified.

In conclusion, the results of our study indicate that ^{18}F-FDG PET/MR is practically equal to ^{18}F-FDG PET/CT for the assessment of HL and aggressive NHLs, regardless of whether or not DWI is included in the protocol. In indolent NHLs, which include those with a variable FDG avidity, the addition of DWI improves the sensitivity and accuracy of ^{18}F-FDG PET/MR and provides results that are superior to those of ^{18}F-FDG PET/CT. The latter observation, in combination with the considerably lower radiation exposure of ^{18}F-FDG PET/MR, may indicate that ^{18}F-FDG PET/MR could possibly replace ^{18}F-FDG PET/CT as the imaging technique of choice in the future, provided that our study results are confirmed by future larger-scale studies.

REFERENCES

1. Meignan M, Gallamini A, Haioun C, et al. Report on the 5th International Workshop on Positron Emission Tomography in Lymphoma held in Menton, France, 19–20 September 2014. *Leuk Lymphoma*. 2015;56:1229–1232.
2. Cheson BD, Fisher RI, Barrington SF, et al. Recommendations for initial evaluation, staging, and response assessment of Hodgkin and non-Hodgkin lymphoma: the Lugano classification. *J Clin Oncol*. 2014;32:3059–3068.
3. Cheson BD. Staging and response assessment in lymphomas: the new Lugano classification. *Chin Clin Oncol*. 2015;4:5.
4. Barrington SF, Mikhaeel NG, Kostakoglu L, et al. Role of imaging in the staging and response assessment of lymphoma: consensus of the International Conference on Malignant Lymphomas Imaging Working Group. *J Clin Oncol*. 2014;32:3048–3058.
5. Kostakoglu L, Cheson BD. Current role of FDG PET/CT in lymphoma. *Eur J Nucl Med Mol Imaging*. 2014;41:1004–1027.
6. Kostakoglu L, Cheson BD. State-of-the-art research on "lymphomas: role of molecular imaging for staging, prognostic evaluation, and treatment response". *Front Oncol*. 2013;3:212.
7. Lin C, Luciani A, Itti E, et al. Whole-body diffusion-weighted magnetic resonance imaging with apparent diffusion coefficient mapping for staging patients with diffuse large B-cell lymphoma. *Eur Radiol*. 2010;20:2027–2038.
8. van Ufford HM, Kwee TC, Beek FJ, et al. Newly diagnosed lymphoma: initial results with whole-body T1-weighted, STIR, and diffusion-weighted MRI compared with ^{18}F-FDG PET/CT. *AJR Am J Roentgenol*. 2011;196:662–669.
9. Abdulqadhr G, Molin D, Aström G, et al. Whole-body diffusion-weighted imaging compared with FDG-PET/CT in staging of lymphoma patients. *Acta Radiol*. 2011;52:173–180.
10. Stéphane V, Samuel B, Vincent D, et al. Comparison of PET-CT and magnetic resonance diffusion weighted imaging with body suppression (DWIBS) for initial staging of malignant lymphomas. *Eur J Radiol*. 2013;82:2011–2017.
11. Gu J, Chan T, Zhang J, et al. Whole-body diffusion-weighted imaging: the added value to whole-body MRI at initial diagnosis of lymphoma. *AJR Am J Roentgenol*. 2011;197:W384–W391.
12. Mayerhoefer ME, Karanikas G, Kletter K, et al. Evaluation of diffusion-weighted MRI for pretherapeutic assessment and staging of lymphoma: results of a prospective study in 140 patients. *Clin Cancer Res*. 2014;20:2984–2993.
13. Mayerhoefer ME, Karanikas G, Kletter K, et al. Evaluation of diffusion-weighted magnetic resonance imaging for follow-up and treatment response assessment of lymphoma: results of an ^{18}F-FDG-PET/CT-controlled prospective study in 64 patients. *Clin Cancer Res*. 2015;21:2506–2513.
14. Runge VM. Current technological advances in magnetic resonance with critical impact for clinical diagnosis and therapy. *Invest Radiol*. 2013;48:869–877.
15. Quick HH, von Gall C, Zeilinger M, et al. Integrated whole-body PET/MR hybrid imaging: clinical experience. *Invest Radiol*. 2013;48:280–289.
16. Grueneisen J, Beiderwellen K, Heusch P, et al. Simultaneous positron emission tomography/magnetic resonance imaging for whole-body staging in patients with recurrent gynecological malignancies of the pelvis: a comparison to whole-body magnetic resonance imaging alone. *Invest Radiol*. 2014;49:808–815.
17. Platzek I, Beuthien-Baumann B, Ordemann R, et al. FDG PET/MR for the assessment of lymph node involvement in lymphoma: initial results and role of diffusion-weighted MR. *Acad Radiol*. 2014;21:1314–1319.
18. Platzek I, Beuthien-Baumann B, Langner J, et al. PET/MR for therapy response evaluation in malignant lymphoma: initial experience. *MAGMA*. 2013;26:49–55.
19. Heacock L, Weissbrot J, Raad R, et al. PET/MRI for the evaluation of patients with lymphoma: initial observations. *AJR Am J Roentgenol*. 2015;204:842–848.
20. Cheson BD. Role of functional imaging in the management of lymphoma. *J Clin Oncol*. 2011;29:1844–1854.
21. Armitage JO. Staging non-Hodgkin lymphoma. *CA Cancer J Clin*. 2005;55:368–376.
22. Lister TA, Crowther D, Sutcliffe SB, et al. Report of a committee convened to discuss the evaluation and staging of patients with Hodgkin's disease: Cotswolds meeting. *J Clin Oncol*. 1989;7:1630–1636.
23. Toledano-Massiah S, Luciani A, Itti E, et al. Whole-body diffusion-weighted imaging in Hodgkin lymphoma and diffuse large B-cell lymphoma. *Radiographics*. 2015;35:747–764.
24. Mayerhoefer ME, Raderer M. Diffusion-weighted MRI for lymphoma staging—response. *Clin Cancer Res*. 2015;21:222–223.
25. Rosenkrantz AB, Oei M, Babb JS, et al. Diffusion-weighted imaging of the abdomen at 3.0 Tesla: image quality and apparent diffusion coefficient reproducibility compared with 1.5 Tesla. *J Magn Reson Imaging*. 2011;33:128–135.
26. Kiliçkesmez O, Yirik G, Bayramoğlu S, et al. Non-breath-hold high b-value diffusion-weighted MRI with parallel imaging technique: apparent diffusion coefficient determination in normal abdominal organs. *Diagn Interv Radiol*. 2008;14:83–87.
27. Bonarelli C, Teixeira PAG, Hossu G, et al. Impact of ROI positioning and lesion morphology on apparent diffusion coefficient analysis for the differentiation between benign and malignant nonfatty soft-tissue lesions. *AJR Am J Roentgenol*. 2015;205:W106–W113.
28. Drzezga A, Souvatzoglou M, Eiber M, et al. First clinical experience with integrated whole-body PET/MR: comparison to PET/CT in patients with oncologic diagnoses. *J Nucl Med*. 2012;53:845–855.
29. Kuhn FP, Hüllner M, Mader CE, et al. Contrast-enhanced PET/MR imaging versus contrast-enhanced PET/CT in head and neck cancer: how much MR information is needed? *J Nucl Med*. 2014;55:551–558.
30. Grueneisen J, Nagarajah J, Buchbender C, et al. Positron emission tomography/magnetic resonance imaging for local tumor staging in patients with primary breast cancer: a comparison with positron emission tomography/computed tomography and magnetic resonance imaging. *Invest Radiol*. 2015;50:505–513.
31. Isaacson PG, Chott A, Nakumura S, et al. Extranodal marginal cell lymphoma of mucosa-associated tissue (MALT lymphoma). In: Swerdlow SH, Campo E, Harris NL, et al., eds. *WHO Classification of Tumours of the Haematopoietic and Lymphoid Tissues*. IARC: Lyon, France; 2008:214–219.
32. Zytoon AA, Murakami K, El-Kholy MR, El-Shorbagy E. Dual time point FDG-PET/CT imaging… Potential tool for diagnosis of breast cancer. *Clin Radiol*. 2008;63:1213–1227.
33. Dirisamer A, Halpern BS, Schima W, et al. Dual-time-point FDG-PET/CT for the detection of hepatic metastases. *Mol Imaging Biol*. 2008;10:335–340.
34. Hu M, Han A, Xing L, et al. Value of dual-time-point FDG PET/CT for mediastinal nodal staging in non-small-cell lung cancer patients with lung comorbidity. *Clin Nucl Med*. 2011;36:429–433.

35. Shinya T, Fujii S, Asakura S, et al. Dual-time-point F-18 FDG PET/CT for evaluation in patients with malignant lymphoma. *Ann Nucl Med*. 2012; 26:616–621.

36. Rakheja R, Chandarana H, DeMello L, et al. Correlation between standardized uptake value and apparent diffusion coefficient of neoplastic lesions evaluated with whole-body simultaneous hybrid PET/MRI. *AJR Am J Roentgenol*. 2013; 201:1115–1119.

37. Wu X, Korkola P, Pertovaara H, et al. No correlation between glucose metabolism and apparent diffusion coefficient in diffuse large B-cell lymphoma: a PET/CT and DW-MRI study. *Eur J Radiol*. 2011;79:e117–e121.

38. Nakajo M, Kajiya Y, Kaneko T, et al. FDG PET/CT and diffusion-weighted imaging for breast cancer: prognostic value of maximum standardized uptake values and apparent diffusion coefficient values of the primary lesion. *Eur J Nucl Med Mol Imaging*. 2010;37:2011–2020.

39. Rubesova E, Grell AS, De Maertelaer V, et al. Quantitative diffusion imaging in breast cancer: a clinical prospective study. *J Magn Reson Imaging*. 2006;24: 319–324.

40. Pickles MD, Gibbs P, Sreenivas M, et al. Diffusion-weighted imaging of normal and malignant prostate tissue at 3.0 T. *J Magn Reson Imaging*. 2006;23:130–134.

41. Naganawa S, Sato C, Kumada H, et al. Apparent diffusion coefficient in cervical cancer of the uterus: comparison with the normal uterine cervix. *Eur Radiol*. 2005; 15:71–78.

42. Punwani S, Prakash V, Bainbridge A, et al. Quantitative diffusion weighted MRI: a functional biomarker of nodal disease in Hodgkin lymphoma? *Cancer Biomark*. 2010;7:249–259.

43. de Jong A, Kwee TC, de Klerk JM, et al. Relationship between pretreatment FDG-PET and diffusion-weighted MRI biomarkers in diffuse large B-cell lymphoma. *Am J Nucl Med Mol Imaging*. 2014;4:231–238.